ELSEVIER

Communication

Fast proton spin-lattice relaxation time in the rotating frame during the application of time averaged precession frequency

Zoran D. Žujović *, Graham A. Bowmaker

Department of Chemistry, The University of Auckland, Private Bag 92019, Auckland, New Zealand

Abstract

A relatively rapid phase alternation of the effective field in the time averaged precession frequency (TAPF) sequence results in averaging of the proton RF spin-lock field. The spin-locking of the proton magnetization becomes less efficient and thus shortens $T_{1\rho}^{H}$, the proton spin-lattice relaxation time in the rotating frame. The relaxation time also depends on the ratio of τ_1 and τ_2 intervals i.e. τ_1/τ_2 and not only on the number of $\tau_c = \tau_1 + \tau_2$ blocks, i.e. the number of the phase transients. Experiments are performed on solid samples of ferrocene and glycine and for some time intervals, $T_{1\rho}^{H}$ is shortened by factors of 9–100 compared to the relaxation times obtained in the standard experiment.
© 2006 Elsevier Inc. All rights reserved.

Keywords: Cross-polarization; TAPF; Rotating frame relaxation

1. Introduction

Cross-polarization (CP) is a double resonance NMR technique that allows transfer of magnetization (or polarization) from abundant or high-γ spins denoted as I (most often ^{1}H) to the rare or low-γ nuclei (^{13}C, ^{29}Si, ^{31}P, ^{15}N...) denoted as S [1]. Besides the fact that CP dramatically increases sensitivity, it also overcomes the other common problem in solid-state NMR, e.g. the long time needed to acquire spectra. In the CP experiment recycle delays are no longer dependent on the spin-lattice relaxation time in the laboratory frame of the spin S (T_1^S) but on T_1^I, the relaxation in the laboratory frame of spin I, which is usually significantly shorter. Thus, sensitivity is improved not only by the transfer of magnetization, but also by a shortening of the experimental time. The basic idea of CP technique is to keep I and S spins-locked simultaneously along the corresponding resonant radio-frequency (RF) fields (B_I and B_S) in a double rotating coordinate frame. The optimum of polarization transfer is attained under the Hartmann–

Hahn condition ($\gamma_I B_I = \gamma_S B_S$), i.e. when both spins have equal nutation frequencies about the RF fields. The intensity of the S spin detected signal depends on the kinetics of transfer of the magnetization. The dynamics of cross-polarization are usually described by a model in which the growth of S spin magnetization is governed by the rate of cross-polarization T_{SI}. However, the rise in rare nucleus magnetization is counteracted by another process: reduction of the proton magnetization due to the relaxation of I spins in the rotating frame (during the spin-lock) with the time constant $T_{1\rho}^I$. This time constant is determined by the spin-diffusion and motional characteristics of the molecules or structural units. On the other hand the T_{SI} time constant depends on S–I dipolar coupling. If this coupling is strong (S spins directly attached to I spins), T_{SI} is very short, resulting in a fast polarization transfer and initial buildup of magnetization. However, for remote S spins not attached to I, or belonging to structural units with significant motion, dipolar coupling becomes relatively weak and T_{SI} is long, resulting in a slow rise of S magnetization [2,3].

Under these circumstances, the S signal will pass through a maximum that is different for each molecular

---

* Corresponding author. Fax: +64 9 373 7422.
E-mail address: z.zujovic@auckland.ac.nz (Z.D. Žujović).

group or structural unit with a different degree of protonation or mobility. Thereafter, the signal will decay with the time constant $T_{1\rho}^I$. It is therefore very difficult (if not impossible) to uniformly polarize all S spins within a particular molecule using a single contact time [3]. Thus, the combination of long T_{SI} and short $T_{1\rho}^I$ relaxation times can make spectral analysis difficult. This is because the S spins that are distant from I spins, or those that are attached to I spins with very short $T_{1\rho}^I$ cannot be completely polarized. In these cases cross-polarized signal intensities are greatly reduced resulting in inaccurate quantitative analysis [3]. From the theoretical point of view, quantitative CP measurements can be performed when $T_{1\rho}^I \gg T_{SI}$. The spin dynamics of cross-polarization has been comprehensively studied elsewhere [2–14].

Beside these intrinsic characteristics of the sample that can influence CP, there are also some other external factors: Hartmann–Hahn mismatching, phase transients, RF field strength etc.

One of the further limitations of the CP pulse sequence is that it requires very strong RF fields for very low-γ nuclei for Hartmann–Hahn matching. For instance, due to the fact that γ for ^{15}N is a factor of about 10 times lower than that of ^{1}H, the strength of the applied RF field in the nitrogen channel must be 10 times higher than that applied in the ^{1}H channel. This problem is very critical for power lossy and heat sensitive biological samples, such as, for example, membrane proteins and peptides, where application of high RF power can denature the samples.

Among the proposed sequences which reduce the required RF field power in the I channel [15–17], the TAPF (time averaged precession frequency) sequence [15] (see Fig. 1A) has proved to be a very useful one. The idea of this sequence is based on the paper of Rhim et al. [18] which proposed the technique of time reversal nutation frequency. This method was used to remove the effects of nutation of a spin isochromat around the effective field during the burst in magic echo sequence by using phase alternating intervals with *equal* durations.

However, unlike the Rhim sequence the TAPF uses *different* duration times (τ_1 and τ_2) for phase alternating periods in the I channel. During these periods the precession of spin isochromats around the effective field is time reversed. Fast alternation averages the precession frequency, so one can control the angle of precession of I spin isochromat about the effective field. The time averaged frequency is:

$$\overline{\omega_{eI}} = \left| \frac{\tau_1 - \tau_2}{\tau_c} \right| \omega_{eI}$$

where $\omega_{eI} = \gamma_I B_{1I}$ and $\tau_c = \tau_1 + \tau_2$. Now, the Hartmann–Hahn condition reads

$$\overline{\omega_{eI}} = \omega_{eS} = \gamma_S B_{eS}$$

where B_{eS} is effective S spin RF field strength and ω_{eS} is the precession of the S spin isochromat about the effective field. In this way one can control the precession frequency of spin I isochromat around the RF field, and reduce this
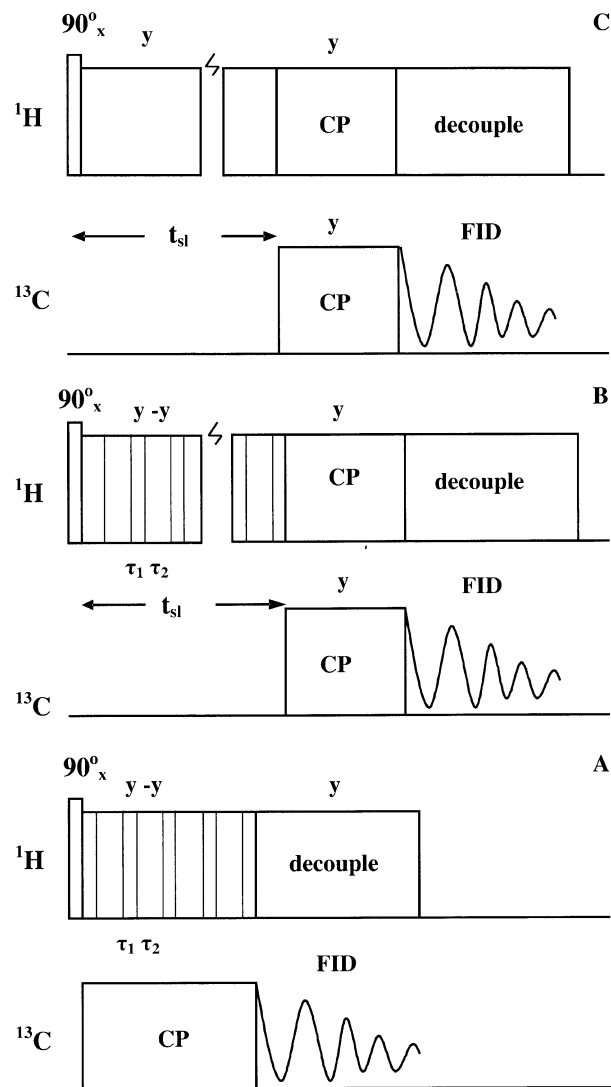

Fig. 1. Pulse sequences used in this work: (A) TAPF sequence, (B) spin-lock with TAPF segment for indirect measurement of $T_{1\rho}^H$ relaxation times and (C) spin-lock in the x-y plane by an on-resonance continuous wave (CW) irradiation for indirect measurement of $T_{1\rho}^H$ relaxation times.

frequency by choosing different time intervals τ_1 and τ_2 with opposite phases. This leads to a significant reduction of the S spin RF field (by up to a factor of 10 [15]).

The scaling factor of the RF field is limited by the correlation time of the dipolar fluctuation in the rotating frame, t_c. This can take any value as long as $\tau_c \ll t_c$ i.e.

$$SC = \frac{\tau_1 - \tau_2}{\tau_c} \leqslant 1$$

For instance, for time intervals τ_1 and τ_2 of 1 and 4 μs the scaling factor is SC = 0.6, while this value for 2 and 3 μs is SC = 0.2. Takegoshi et al. have found that τ_c of 5 μs is short enough to fulfill the condition $\tau_c \ll t_c$, even for rigid crystalline solids with strong dipolar interaction.

Although this is well known and mostly used as a sequence for enhancing sensitivity of S spins at lower RF fields, recent papers showed the applicability of the TAPF sequence to separated local field spectroscopy [19–23]. It is

worth mentioning here that the above equations are valid for time averaging of the effective field and could be readily applied for polarization transfer. If this concept is applied to separated local field (SLF) spectroscopy, the fact that the zero-quantum term of the heteronuclear dipolar interaction does not commute with the difference of the effective fields should be taken into consideration [20].

To the best of our knowledge, none of the published papers have yet addressed the I spin relaxation in the rotating coordinate frame when the TAPF sequence with fast phase alternation is applied during the contact time. It is not our intention to investigate spin dynamics by using the $T_{1\rho}^{H}$ relaxation. Rather, we demonstrate the significant effect of the time averaging of precession frequency (TAPF) by using model substances very often used in solid-state NMR. In this communication, we report the dramatic shortening of $T_{1\rho}^{I}$ relaxation times when the TAPF sequence is applied in the I channel. As pointed out above, this parameter is very important during the transfer of polarization and its neglect can lead to a serious intensity deterioration in CP spectra.

2. Results and discussion

Powder spectra of ferrocene $Fe(C_5H_5)_2$ (Fig. 2), and glycine (Fig. 3) have been widely used in NMR studies of polarization transfer, and these were used in the present study. In the case of ferrocene, the fast molecular rotation of the C_5H_5 ring about its C_5 axis causes its internal homonuclear and heteronuclear dipolar interactions to be reduced by factor of 2 [24,25]. This also causes a significant reduction in the dipolar interactions between adjacent rings. Furthermore, the on-resonance RF irradiation scales down the proton homonuclear dipolar interaction by 1/2. Due to very fast rotations which average out dipolar interactions, ferrocene has a relatively long $T_{1\rho}^{H}$ time at RF field of ≈ 60 kHz.

Glycine $(C_2H_5NO_2)$ is structurally the simplest amino acid. For nuclear magnetic resonance spectroscopists, glycine often serves as a standard for checking and calibrating
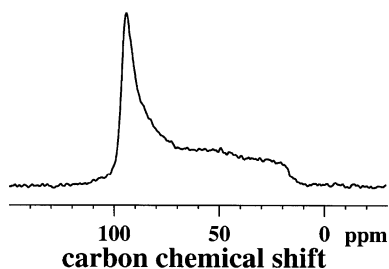
Fig. 2. Carbon spectrum of a powder sample of ferrocene. The spectrum was obtained at ambient temperature on a 300-MHz Bruker Avance spectrometer equipped with a 7-mm MAS probe operated in the static mode at 75.468 MHz ^{13}C frequency. ^{1}H and ^{13}C RF fields, $\gamma B_{1I}/2\pi$ and $\gamma B_{1S}/2\pi$, were set to 59.5 kHz, satisfying the Hartmann–Hahn condition. The number of scans was eight with a 25 s recycle delay. Contact time was 5 ms and sweep width 39.920 kHz.
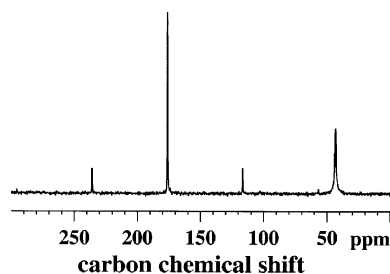
Fig. 3. Carbon spectrum of a sample of glycine. The spectrum was obtained at ambient temperature on a 300-MHz Bruker Avance spectrometer equipped with a 7-mm MAS probe operated at 75.468 MHz ^{13}C frequency. ^{1}H and ^{13}C RF fields, $\gamma B_{1I}/2\pi$ and $\gamma B_{1S}/2\pi$, were set to 59.5 kHz, satisfying the Hartmann–Hahn condition. The number of scans was eight with a 5 s recycle delay. Contact time was 1 ms and sweep width 39.9 kHz. Spinning frequency was 4000 ± 1 Hz.

spectrometer performance. It has been shown that $T_{1\rho}^{H}$ in glycine is 44 ms [26].

The relaxation sequences used in this work are shown in Fig. 1B and C. The sequence shown in Fig. 1C is a standard (continuous wave) proton relaxation experiment in the rotating frame of reference with carbon detection [27]. At the beginning of the sequence, the ^{1}H magnetization is rotated from the z axis to the y axis in the rotating frame by a 90° pulse and then spin-locked along the y axis by continuous wave on-resonance irradiation. The carbon signals are then polarized by cross-polarization and detected during the high power proton decoupling.

Thus, the proton magnetization as a function of spin-lock time t_{sl} can be indirectly monitored by the carbon signal intensities. The concept of the sequence shown in Fig. 1B is the same, except that the spin-locking part before the CP segment now consists of TAPF intervals instead of continuous irradiation as in the standard $T_{1\rho}^{H}$ experiment (see Fig. 1C). The ^{1}H relaxation measurements in the rotating frame of coordinates for a powder sample of ferrocene are shown in Fig. 4.

The relaxation data for ferrocene (especially for the standard relaxation experiment) do not cover the full relaxation of signal intensity and therefore, the long $T_{1\rho}^{H}$ component cannot be established explicitly. Even so, the relaxation data obtained during the first 50 ms of spin-locking, Table 1, give indications of the relative effect of the fast phase alternation. By fitting the experimental data with two components (to get a better fit) up to 50 ms spin-locking time, it is found that the longer component of the measured $T_{1\rho}^{H}$ for ferrocene is ≈ 270 ms. However, in experiments that include TAPF, i.e. fast phase alternation, spin-lattice relaxation times in the rotating frame of coordinates become shorter. The shortening is especially significant for the segment with intervals of $\tau_1 = 3$ μs and $\tau_2 = 2$ μs. In this case, the $T_{1\rho}^{H}$ relaxation time becomes ≈ 30 ms i.e. it is shortened ≈ 9 times compared to that obtained in the standard experiment (270 ms).

The relaxation data for glycine are shown in Fig. 5 and the resulting $T_{1\rho}^{H}$ values are listed in Table 1. This shows that the trend of shortening $T_{1\rho}^{H}$ is more dramatic than
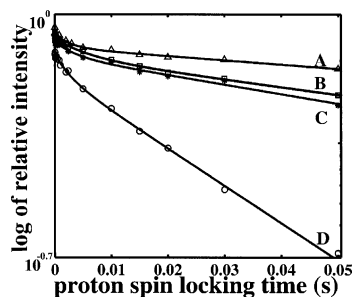
Fig. 4. Semilog plot of normalized magnetization intensities of the peak at 94.4 ppm in ferrocene as a function of the proton spin-locking time using the sequences shown in Fig. 1(B and C). The RF field strength during the variable time proton spin-locking was 59.5 kHz. The experimental conditions are the same as in Fig. 1. (A). Data obtained from continuous spin-locking experiment. For the relaxation experiments with TAPF segment time intervals τ_1 and τ_2 were 4 μs and 1 μs (B), 3 μs and 1 μs (C), and 3 μs and 2 μs, (D).

Table 1
Proton spin-lattice relaxation time in the rotating coordinate frame obtained from experiments (1B TAPF spin-lock) and (1C continuous wave spin-lock) for ferrocene and glycine samples

Segment		$T_{1\rho}^H$ (ms)		
τ_1 (μs)	τ_2 (μs)	Ferrocene		Glycine
4	1	150 (85%)	6 (15%)	27
3	1	123 (85%)	4 (15%)	16
3	2	30 (85%)	3 (15%)	0.5
Continuous spin-lock		270 (90%)	27 (10%)	50

The % in brackets for the ferrocene sample denote the contributions from two components obtained after fitting.
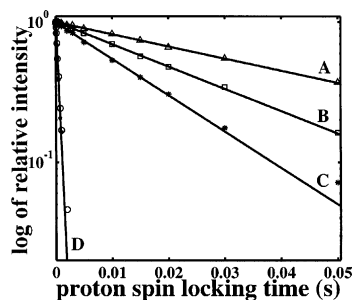

Fig. 5. Semilog plot of normalized magnetization intensities of the peak at 178 ppm (glycine) as a function of the proton spin-locking time using the sequences shown in Fig. 1(B and C). The RF field strength during the variable time proton spin-locking was 59.5 kHz. The experimental conditions are the same as in Fig. 1. (A). Data obtained from continuous spin-locking experiment. For the relaxation experiments with TAPF segment time intervals τ_1 and τ_2 were 4 μs and 1 μs (B), 3 μs and 1 μs (C), and 3 μs and 2 μs, (D).

for the sample of ferrocene. The drastic shortening is observed for the segment with $\tau_1 = 3$ μs and $\tau_2 = 2$ μs. $T_{1\rho}^H$ is shortened from 50 ms (standard experiment) to 0.5 ms, i.e. by factor 100.

The observed shortenings are not so critical for ferrocene, considering its original long $T_{1\rho}^H$. However, in the case of glycine where this shortenings goes up to 100 times and perhaps for some other organic solids where the $T_{1\rho}^H$ time

varies between 1 and 10 ms, this effect could be critical in getting quantitative results, or correct spectra in terms of individual peak intensities.

It is worth noting that the above is analogous to the well known PISEMA sequence [28–30].

In the case of spin-locking at the magic angle (Lee–Goldburg condition-LG) [31,32], the homonuclear interactions are suppressed to first order. Thus, the spin-lock field becomes more effective, resulting in slower relaxation [33,34]. However, introduction of the flip-flop, i.e. frequency-switching (FS) of the Lee–Goldburg segments (PISEMA) [28] shortens the relaxation time, even though the homonuclear decoupling is more effective. The frequency of RF irradiation in the ^1H channel is switched between two LG conditions after 2π rotation of the proton magnetization about the effective field. Along with each frequency switch a phase shift of π is required. Unlike the TAPF, PISEMA has two segments t_{LG} of equal and longer duration than we have used here for the TAPF. For example for RF field amplitude of 59.5 kHz the duration of one LG unit should be $t_{LG} \approx 14$ μs. As discussed by Fu et al. [33,34] the relative shortening in the PISEMA is most probably produced by the phase transients that lead to averaging of the spin-locking field resulting in inefficient locking and dephasing of the magnetization, and eventually to faster $T_{1\rho}^H$ relaxation. These authors found that $T_{1\rho}^H$ in the tilted rotating frame under the FSLG sequence using 2π rotation was twice as short as that using 4π rotation. Thus, in this case for a given spin-lock time, more cycles mean that the effective field alternates its direction more frequently resulting in faster magnetization decay. So, at an RF field of 59.5 kHz and $\tau_1 = 3$ μs and $\tau_2 = 2$ μs, the TAPF experiment introduces more phase switching ($\tau_c = 5$ μs) per unit of time than PISEMA ($2t_{LG} = 28$ μs), and consequently the spin-lock field should be more efficiently averaged.

However, our preliminary results here indicate that this is not completely the case with the TAPF sequence. As can be seen from Table 1 and Figs. 4 and 5 the dramatic shortening is obtained for the time intervals of $\tau_1 = 3$ μs and $\tau_2 = 2$ μs for which $\tau_c = 5$ μs. At the same time for $\tau_1 = 1$ μs and $\tau_2 = 4$ μs ($\tau_c = 5$ μs, as well), the reduction of the relaxation time is not that drastic, although there are the same number of τ_c blocks in both experiments. That means that in our case relaxation time could depend on the ratio of τ_1 and τ_2 intervals i.e. τ_1/τ_2 and not only on the number of τ_c blocks, i.e. the number of the phase transients. Furthermore, in the paper of Nishimura and Naito [35] a new approach to reduce RF power in both ^1H and ^{13}C channels is proposed. This is achieved by alternating the directions of the effective fields for ^1H with unequal duration and amplitudes during the spin exchange.

Therefore, in terms of relaxation times, care should be taken for each particular experiment with a specific type of phase alternation [35–38]. For instance, a new sequence (HIMSELF) to measure heteronuclear dipolar coupling is reported [38]. To suppress chemical shift and homonuclear

dipolar interactions, the BLEW [39] segment is applied in both RF channels. BLEW-12 consists of 12 back-to-back 90° pulses which means that this sequence has also fast phase alternation comparing to PISEMA and relatively similar to TAPF experiments reported here. Our investigation was focused on TAPF with relatively rapid, unequal phase alternated time periods at medium RF power levels.

In conclusion, a relatively rapid phase alternation of the effective field in the TAPF sequence results in averaging of the RF spin-lock field, so the spin-locking of the proton magnetization becomes less efficient and thus shortens the spin-lattice relaxation time $T_{1\rho}^{\mathrm{H}}$ in the rotating frame. The relaxation time depends also on the ratio of τ_1 and τ_2 intervals (τ_1/τ_2). One of the possibilities for reducing phase transient effects is a tune up procedure that should be systematically performed before applying TAPF experiment [40].

Further investigations involving the measurement of $T_{1\rho}^{\mathrm{H}}$ for different τ_c and RF field strength and offset are underway in our laboratory.

Acknowledgments

References

[1] A. Pines, M.G. Gibby, J.S. Waugh, Proton-enhanced NMR of dilute spins in solids, J. Chem. Phys. 59 (1973) 569–590.
[2] M.H. Levitt, D. Suter, R.R. Ernst, Spin dynamics and thermodynamics in solid state NMR cross-polarization, J. Chem. Phys. 84 (1986) 4243–4255.
[3] L.B. Alemany, D.M. Grant, R.J. Pugmire, T.D. Alger, K.W. Zilm, Cross-polarization and magic-angle spinning NMR spectra of model organic compounds, 2. Molecules of low or remote protonation, J. Am. Chem. Soc. 105 (1983) 2143–2147.
[4] X. Wu, S. Zhang, X. Wu, Two stage feature of Hartmann–Hahn cross relaxation in magic-angle sample spinning, Phys. Rev. Ser. B 37 (1988) 9827–9829.
[5] Z. Gan, Spin dynamics of polarization inversion spin exchange at the magic angle in multiple spin system, J. Magn. Reson. 143 (2000) 136–143.
[6] T.N. Venkatraman, N. Sinha, K.V. Ramanathan, Cross-polarization from the dipolar reservoir under the mismatched Hartmann–Hahn condition, J. Magn. Reson. 157 (2002) 137–140.
[7] X. Wu, S. Zhang, Selective polarization inversion and depolarization of ^{13}C in cross relaxation in nmr, Chem. Phys. Lett. 156 (1989) 79–81.
[8] D. Sakellariou, P. Hodgkinson, S. Hediger, L. Emsley, Experimental observation of periodic quasi-equilibria in solid-state NMR, Chem. Phys. Lett. 308 (1999) 381–389.
[9] X. Wu, K.W. Zilm, Heterogeneity of cross relaxation in solid state NMR, J. Magn. Reson. 93 (1991) 265–278.
[10] D. Sakellariou, P. Hodgkinson, L. Emsley, Quasi-equilibria in solid-state NMR, Chem. Phys. Lett. 293 (1998) 110–118.
[11] S. Zhang, Quasi-adiabatic polarization transfer in solid-state NMR, J. Magn. Reson. Ser. A 110 (1994) 73–76.
[12] A. Naito, C.A. McDowell, Anisotropic behavior of the ^{13}C nuclear spin dynamics in a single crystal of L-alanine, J. Chem. Phys. 84 (1986) 4181–4185.
[13] S.C. Shekar, A. Ramamoorthy, The unitary evolution operator for cross-polarization schemes in NMR, Chem. Phys. Lett. 342 (2001) 127–134.
[14] S.C. Shekar, D.K. Lee, A. Ramamoorthy, Chemical shift anisotropy and offset effects in cross polarization solid-state NMR spectroscopy, J. Magn. Reson. 157 (2002) 223–234.
[15] K. Takegoshi, C.A. McDowell, Cross polarization using a time averaged precession frequency. A simple technique to reduce radiofrequency power requirements for magnetization transfer experiments in solids, J. Magn. Reson. 67 (1986) 356–361.
[16] A. Bax, B.L. Hawkins, G.E. Maciel, Off-resonance cross-polarization: a technique to reduce rf power requirements for magnetization transfer experiments in solids, J. Magn. Reson. 59 (1984) 530–535.
[17] S.C. Shekar, D. Lee, A. Ramamoorthy, An experimental strategy to dramatically reduce RF power used in cross polarization solid-state NMR spectroscopy, J. Am. Chem. Soc. 123 (2001) 7467–7468.
[18] W.-K. Rhim, A. Pines, J.S. Waugh, Time-reversal experiments in dipolar coupled systems, Phys. Rev. B 3 (1971) 684.
[19] Z.D. Zujovic, G.A. Bowmaker, C. Mayer, Transient oscillations under strongly mismatched Hartmann–Hahn conditions, J. Magn. Reson. 164 (2003) 358–364.
[20] K. Nishimura, A. Naito, Reduction of rf power of observed nuclei for ^{1}H-homonuclear decoupled cross-polarization in solid-state NMR spectroscopy, Chem. Phys. Lett. 380 (2003) 569–576.
[21] K. Nishimura, A. Naito, Dramatic reduction of the RF power for attenuation of sample heating in 2D-separated local field solid-state NMR spectroscopy, Chem. Phys. Lett. 402 (2005) 245–250.
[22] D.K. Lee, T. Narasimhaswamy, A. Ramamoorthy, PITANSEMA, a low power PISEMA solid state NMR experiment, Chem. Phys. Lett. 399 (2004) 359–362.
[23] K. Yamamoto, V.L. Ermakov, D.K. Lee, A. Ramamoorthy, PITANSEMA-MAS, a solid-state NMR method to measure heteronuclear dipolar couplings under MAS, Chem. Phys. Lett. 408 (2005) 118–122.
[24] S. Zhang, B.H. Meier, R.R. Ernst, Mismatch-compensated cross polarization. W-MOIST, an improved pulse scheme, J. Magn. Reson. Ser. A 108 (1994) 30–37.
[25] K.J. Hallock, D.K. Lee, A. Ramamoorthy, Carbon-13 chemical shifts and ^{1}H-^{13}C dipolar couplings in metal sandwich solids using one-dimensional solid-state NMR spectroscopy, Chem. Phys. Lett. 302 (1999) 175–180.
[26] R.E. Taylor, ^{13}C CP/MAS: application to glycine, Concepts Magn. Reson. 22A (2) (2004) 72–79.
[27] E.O. Stejskal, J.D. Memory, High Resolution NMR in the Solid State. Fundamentals of CP/MAS, University Press, Oxford, 1994.
[28] C.H. Wu, A. Ramamoorthy, S.J. Opella, High resolution heteronuclear dipolar solid-state NMR spectroscopy, J. Magn. Reson. 109 (1994) 270–272.
[29] K. Yamamoto, D.K. Lee, A. Ramamoorthy, Broadband-PISEMA solid-state NMR spectroscopy, Chem. Phys. Lett. 407 (2005) 289–293.
[30] A. Ramamoorthy, Y. Wei, D.K. Lee, EPISEMA solid-state NMR spectroscopy, Ann. Rep. NMR Spectorscopy 52 (2004) 1–52.
[31] R.K. Hester, V.R. Cross, L.L. Ackerman, J.S. Waugh, Resolved dipolar coupling spectra of dilute nuclear spins in solids, Phys. Rev. Lett. 34 (1975) 993–995.
[32] R.K. Hester, V.R. Cross, L.L. Ackerman, J.S. Waugh, Structure determination by dipolar coupling measurements of dilute nuclear spins in a polycrystalline solid, J. Chem. Phys. 63 (1975) 3606–3608.
[33] R. Fu, C. Tian, T.A. Cross, NMR spin locking of proton magnetization under a frequency-switched Lee–Goldburg pulse sequence, J. Magn. Reson. 154 (2002) 130–135.
[34] R. Fu, J. Hu, T.A. Cross, Towards quantitative measurements in solid-state CPMAS NMR: a Lee–Goldburg frequency modulated cross-polarization scheme, J. Magn. Reson. 168 (2004) 8–17.

[35] K. Nishimura, A. Naito, Remarkable reduction of rf power by ATANSEMA and DATANSEMA separated local field in solid-state NMR spectrsocopy, Chem. Phys. Lett. 419 (2006) 120–124.

[36] A.A. Nevzorov, S.J. Opella, A "Magic sandwich" pulse sequence with reduced offset dependence for high-resolution separated local field spectroscopy, J. Magn. Reson. 164 (2003) 182–186.

[37] S.V. Dvinskikh, K. Yamamoto, A. Ramamoorthy, Separated local field NMR spectroscopy by windowless isotropic mixing, Chem. Phys Lett. 419 (2006) 168–173.

[38] K. Yamamoto, S.V. Dvinskikh, A. Ramamoorthy, Measurement of heteronuclear dipolar couplings using a rotating frame solid-state NMR experiment, Chem. Phys Lett. 419 (2006) 533–536.

[39] D.P. Burum, M. Linder, R.R. Ernst, Low-power multipulse line narrowing in solid-state NMR, J. Magn. Reson. 44 (1981) 173–188.

[40] A. Ramamoorthy, C.H. Wu, S.J. Opella, Experimental aspects of multidimensional solid-state NMR correlation spectroscopy, J. Magn. Reson. 140 (1999) 131–140.